A COMBINATION TECHNIQUE FOR THE SOLUTION OF SPARSE GRID PROBLEMS

MICHAEL GRIEBEL, MICHAEL SCHNEIDER, CHRISTOPH ZENGER*

Abstract. Two-dimensional sparse grids contain only $O(h^{-1}\log(h^{-1}))$ grid points, in contrast to the usually used full $O(h^{-2})$-grids, whereas for a sufficiently smooth function the accuracy of the representation is only slightly deteriorated from $O(h^2)$ to $O(h^2\log(h^{-1}))$.

The combination technique presented in this paper uses the solutions of $O(\log(h^{-1}))$ different, on regular standard grids discretized problems with $O(h^{-1})$ grid points and e.g. different mesh sizes in the x- and y-direction to produce a sparse grid solution. Assuming a sufficiently smooth solution and asymptotic error expansions for the different discrete solutions, it is shown that the leading error terms are cancelled by the combination technique, and a sparse grid solution with an accuracy of the order $O(h^2\log(h^{-1}))$ is created.

The proof is extended to the three-dimensional case. Here, by the combination of $O((\log(h^{-1}))^2)$ solutions on different grids with $O(h^{-1})$ grid points, an accuracy of the order $O(h^2(\log(h^{-1}))^2)$ is achieved.

Additionally, the results of numerical experiments are reported. There, it can be seen that the combination approach works not only for sufficiently smooth solutions of linear problems, but, to some extent, also for non-smooth solutions and even for non-linear problems.

1. Grids and Spaces. Let $\Omega_{i,j}$ be the equidistant rectangular grid on the unit square $\Omega = [0,1]\times[0,1]$ with meshwidth $h_i = 2^{-i}$ in x- and $h_j = 2^{-j}$ in y-direction. Let moreover $S_{i,j}$ be the space of piecewise bilinear functions on grid $\Omega_{i,j}$.

A partial differential equation $Lu = f$ with appropriate boundary conditions can now be discretized on any grid $\Omega_{i,j}$ using the finite element method and standard basis functions. For reasons of simplicity we only consider homogeneous Dirichlet boundary conditions and restrict the space $S_{i,j}$ to the space $S^0_{i,j}$ of functions that satisfy these boundary conditions.

The associated discrete problem $P_{i,j}$ is then described by

$$L_{i,j}u_{i,j} = f_{i,j},$$

where $u_{i,j}$ denotes the computed finite element solution represented in the standard basis of pagoda functions.

The different grids, mesh sizes, spaces, problems and solutions are now uniquely described by the index pairs (i,j), $i,j = 1,2,3,\ldots$. The associated grids are represented in figure 1.

For the representation of the problems $P_{i,j}$ and solutions $u_{i,j}$ we can also choose the product-type hierarchical basis of [6] instead of the standard basis.

There, the finite element space $S^0_{i,j}$ of piecewise bilinear functions on grid $\Omega_{i,j}$ that satisfy the boundary conditions is decomposed by

$$S^0_{i,j} \;=\; \sum_{s=1}^{i}\sum_{t=1}^{j} T_{s,t},$$

where $T_{s,t}$ denotes the subspace of $S^0_{s,t}$ vanishing on all grid points corresponding to the grids of $S^0_{s-1,t}$ and $S^0_{s,t-1}$. We can introduce bilinear basis functions in $T_{s,t}$ that are uniquely described by their non-overlapping rectangular support of size $1/2^{s-1}$ in x- and $1/2^{t-1}$ in y-direction. This results in a product-type hierarchical basis. For a more detailed description see [6] or [1], figure 2.

* Institut für Informatik, Technische Universität München, Arcisstraße 21, D-8000 München 2

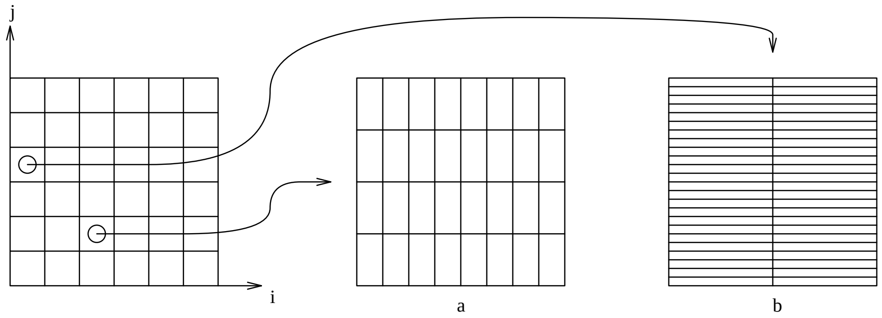

FIG. 1. *Diagram of grids (examples: $\Omega_{3,2}$ (a), $\Omega_{1,4}$ (b)).*

Then every $u \in S^0_{i,j}$ is represented by

$$u = \sum_{s=1}^{i} \sum_{t=1}^{j} u_{s,t}, \quad \text{where} \quad u_{s,t} \in T_{s,t}, \; s = 1, \dots, i, \; t = 1, \dots, j.$$

Using this type of hierarchical basis the calculation with functions defined on different grids and spaces is simplified. For example, the addition of two functions defined on different grids is reduced to the addition of the single coefficients. This is due to the fact that now the basis functions that are associated with the grid points which belong to both grids are just the same.

The transformation of the coefficients $u_{s,t}$ of a function on grid $\Omega_{i,j}$ represented in standard basis to its representation in hierarchical basis can be implemented by a constant number of operations per grid point. To this end assume that the values of u on grid $\Omega_{i,j}$ represented in standard basis are stored in an array $U[0:N, 0:M]$, where $N = 2^i$ and $M = 2^j$. The transformation to the hierarchical basis representation is done by the algorithm shown in figure 2.

```
integer lx,ly,hx,hy,x,y
real U[0:N,0:M]
for ly=1 to j step 1
    hy = 2^(ly-1)
    for x=0 to N step 1
        for y=hy to M-hy step 2hy
            U[x,y] = U[x,y]-(U[x,y-hy]+U[x,y+hy])/2
        endfor
    endfor
endfor
for lx=1 to i step 1
    hx = 2^(lx-1)
    for y=0 to M step 1
        for x=hx to N-hx step 2hx
            U[x,y] = U[x,y]-(U[x-hx,y]+U[x+hx,y])/2
        endfor
    endfor
endfor
```

FIG. 2. *Transformation to the hierarchical basis representation.*

This gives further insight to our hierarchical basis. Note that the program of figure 2 also works for non-homogeneous boundary conditions.

The transformation is associated with the stencil

$$\begin{bmatrix} -1/2 \\ 1 \\ -1/2 \end{bmatrix} * \begin{bmatrix} -1/2 & 1 & -1/2 \end{bmatrix} = \begin{bmatrix} 1/4 & -1/2 & 1/4 \\ -1/2 & 1 & -1/2 \\ 1/4 & -1/2 & 1/4 \end{bmatrix},$$

where the size of the stencil is just the support of the associated hierarchical basis function from $T_{i,j}$. This stencil is the standard difference approximation of $\frac{h_i^2 h_j^2}{4} \frac{\partial^4 u}{\partial x^2 \partial y^2}$. Note that the transformation can be inverted easily.

Following [6], we now define the seminorm

$$|u| \;=\; \|\frac{\partial^4 u}{\partial x^2 \partial y^2}\|_\infty$$

on the space of functions u on Ω where $\frac{\delta^4 u}{\delta x^2 \delta y^2}$ exists, and is continuous. Let now $u_{i,j}^I$ be the interpolant of u into $S_{i,j}^0$ represented in hierarchical basis

$$u_{i,j}^I \;=\; \sum_{s=1}^{i} \sum_{t=1}^{j} u_{s,t} \quad \text{with} \quad u_{s,t} \in T_{s,t} \; .$$

We learned in [6] (see (2.5)) that for the coefficients the estimation

$$\|u_{s,t}\|_\infty \;\leq\; 4^{-s-t-1}\;|u|$$

is valid. This is a just a property of the representation in the product-type hierarchical basis. For the interpolation error we get as in [6]

$$\begin{aligned}
\|u - u_{i,j}^I\|_\infty &= \|\sum_{s=1}^{\infty}\sum_{t=1}^{\infty} u_{s,t} \;-\; \sum_{s=1}^{i}\sum_{t=1}^{j} u_{s,t}\|_\infty \\
&\leq \sum_{s=1}^{i}\sum_{t=j+1}^{\infty} \|u_{s,t}\|_\infty + \sum_{s=i+1}^{\infty}\sum_{t=1}^{j} \|u_{s,t}\|_\infty + \sum_{s=i+1}^{\infty}\sum_{t=j+1}^{\infty} \|u_{s,t}\|_\infty \\
&\leq \frac{1}{4}|u| \left(\sum_{s=1}^{i}\sum_{t=j+1}^{\infty} 4^{-s-t} + \sum_{s=i+1}^{\infty}\sum_{t=1}^{j} 4^{-s-t} + \sum_{s=i+1}^{\infty}\sum_{t=j+1}^{\infty} 4^{-s-t} \right) \\
&= \frac{1}{36}|u| \Big((1-4^{-i}) * 4^{-j} + 4^{-i} * (1-4^{-j}) + 4^{-i-j} \Big) \\
&= \frac{1}{36}|u| (h_i^2 + h_j^2 - h_i^2 h_j^2).
\end{aligned}$$

Thus, the order of convergence is $O(h_i^2 + h_j^2)$.

2. Sparse Grid Spaces and Functions and a Combination of Interpolants. Following the argumentation in [6], we use as our finite element space the direct sum of the subspaces where the contribution to the error is equal or larger than some prescribed tolerance (we choose here $4^{-n-2}|u|$) and omit the rest. This leads to a triangular scheme of subspaces $T_{i,j}$ with $i + j \leq n + 1$, and results in an approximation space that corresponds to a "sparse" grid instead of a "full" grid.

The sparse grid space of functions that satisfy the boundary condition is defined as

$$\hat{S}_{n,n}^0 \;=\; \sum_{s=1}^{n} \sum_{t=1}^{n-s+1} T_{s,t} \quad = \sum_{s+t \leq n+1} T_{s,t} \; .$$

Let now

$$\hat{u}^I_{n,n} \;=\; \sum_{s=1}^{n} \sum_{t=1}^{n-s+1} u_{s,t} \quad \text{with } u_{s,t} \in T_{s,t}$$

be the interpolant of u into $\hat{S}^0_{n,n}$. The interpolation error of the sparse grid space is bounded by

$$\|u - \hat{u}^I_{n,n}\|_\infty \;\le\; \frac{1}{48}\,|u|\,h_n^2\,(ld(h_n^{-1}) \;+\; \frac{4}{3})\,.$$

For the detailed proof see (2.9) in [6].

Altogether, we see that the use of the sparse grid space $\hat{S}^0_{n,n}$ instead of the usual "full" space $S^0_{n,n}$ reduces the dimension from $O(h_n^{-2})$ to $O(h_n^{-1}\log(h_n^{-1}))$. The accuracy, however, is only deteriorated from $O(h_n^2)$ to $O(h_n^2\log(h_n^{-1}))$.

Now, we will give a different motivation of the sparse grid approach. To this end, we seek a certain linear combination of **full** grid spaces $S^0_{i,j}$ so that the sparse grid space is created.

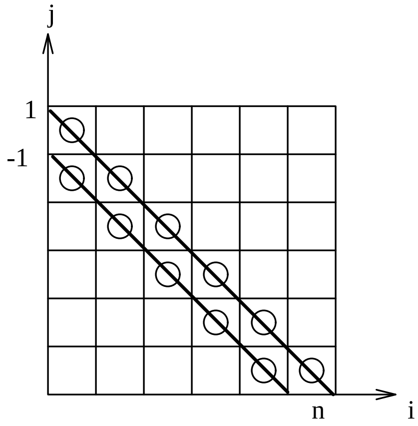

FIG. 3. *The linear combination of regular "full" grid functions.*

It is easy to see that for the interpolant $\hat{u}^I_{n,n}$ the following equation holds:

$$\hat{u}^I_{n,n} \;=\; \sum_{i+j=n+1} u^I_{i,j} \;-\; \sum_{i+j=n} u^I_{i,j}.$$

Thus, the interpolant $\hat{u}^I_{n,n}$ of u into the sparse grid space $\hat{S}^0_{n,n}$ is just a linear combination of the interpolants of u into the full grid spaces $S_{i,j},\ i+j=n,n+1$.

This linear combination is visualized in figure 3.

This gives the idea to represent any sparse grid function as a linear combination of its interpolants on the regular full grids $\Omega_{i,j},\ i+j=n,n+1$. This approach has the advantage that only regular data structures must be used. There is no need for more complicated data structures than a few arrays to store a sparse grid function.

3. The Combination of the Solutions of the Problems. Now we consider directly the combination of the FE-solutions

$$\hat{u}^c_{n,n} \;:=\; \sum_{i+j=n+1} u_{i,j} \;-\; \sum_{i+j=n} u_{i,j}\;.$$

This is a function on the sparse grid space $\hat{S}^0_{n,n}$, but in general $\hat{u}^c_{n,n}$ is **not equal** to the solution $\hat{u}_{n,n}$ of the FE-problem on the sparse grid. Therefore, a proof using the upper bound error estimation of the interpolation error like in chapter 2 is not possible. We will use asymptotic error expansions instead. For smooth functions we show that the error $u - \hat{u}^c_{n,n}$ is of the same order $O(h_n^2 \log(h_n^{-1}))$ as the interpolation error $u - \hat{u}^I_{n,n}$.

To this end assume that the exact solution u is sufficiently smooth and that for every discrete solution $u_{i,j}$, $i, j = 1, 2, 3, \ldots$, pointwise an error expansion of the type

$$u - u_{i,j} \;=\; C_1(h_i)h_i^2 \;+\; C_2(h_j)h_j^2 \;+\; D(h_i, h_j)h_i^2 h_j^2$$

exists, where C_1, C_2 and D are appropriate coefficient functions that are bounded from above by a positive constant κ, i.e. $|C_1(h_i)| \leq \kappa$, $|C_2(h_j)| \leq \kappa$, $|D(h_i, h_j)| \leq \kappa \;\forall h_i, h_j$. This asymptotic expansion holds e.g. for Poisson's problem on a rectangular domain with sufficiently smooth Dirichlet or Neumann boundary conditions and a sufficiently smooth right hand side. For the Laplace equation on the equidistant uniform grid a first proof of the existence of such an expansion was given in [4]. This proof was recently extended to anisotropic grids, with different mesh sizes in the x- and y-direction. See [5] for further details.

Consider now the error of the combined solution $u - \hat{u}^c_{n,n}$. We have

$$\begin{aligned} u - \hat{u}^c_{n,n} &= u - \sum_{i+j=n+1} u_{i,j} + \sum_{i+j=n} u_{i,j} \\ &= \sum_{i+j=n+1} (u - u_{i,j}) - \sum_{i+j=n} (u - u_{i,j}), \end{aligned}$$

and with the error expansion above we get

$$\begin{aligned} u - \hat{u}^c_{n,n} &= \sum_{i+j=n+1} \big(C_1(h_i)h_i^2 + C_2(h_j)h_j^2 + D(h_i, h_j)h_i^2 h_j^2\big) \\ &\quad - \sum_{i+j=n} \big(C_1(h_i)h_i^2 + C_2(h_j)h_j^2 + D(h_i, h_j)h_i^2 h_j^2\big) \\ &= \sum_{i=1}^{n} C_1(h_i)h_i^2 - \sum_{i=1}^{n-1} C_1(h_i)h_i^2 \\ &\quad + \sum_{j=1}^{n} C_2(h_j)h_j^2 - \sum_{j=1}^{n-1} C_2(h_j)h_j^2 \\ &\quad + \sum_{i+j=n+1} D(h_i, h_j)h_i^2 h_j^2 - \sum_{i+j=n} D(h_i, h_j)h_i^2 h_j^2 \\ &= \left(C_1(h_n) + C_2(h_n) + \frac{1}{4} \sum_{i+j=n+1} D(h_i, h_j) - \sum_{i+j=n} D(h_i, h_j) \right) h_n^2 \,. \end{aligned}$$

This leads to the estimation

$$\begin{aligned} |u - \hat{u}^c_{n,n}| &\leq |C_1(h_n)|h_n^2 + |C_2(h_n)|h_n^2 \\ &\quad + |\frac{1}{4} \sum_{i+j=n+1} D(h_i, h_j) - \sum_{i+j=n} D(h_i, h_j)| \; h_n^2 \end{aligned}$$

$$
\begin{aligned}
&\le |C_1(h_n)|h_n^2 \;+\; |C_2(h_n)|h_n^2 \\
&+ \frac{1}{4} \sum_{i+j=n+1} |D(h_i,h_j)|h_n^2 \;+\; \sum_{i+j=n} |D(h_i,h_j)|h_n^2 \\
&\le \kappa h_n^2 \;+\; \kappa h_n^2 \;+\; \frac{1}{4}\kappa n h_n^2 \;+\; \kappa(n-1)h_n^2 \\
&= \kappa h_n^2 (1 + \frac{5}{4} n) \\
&= \kappa h_n^2 (1 + \frac{5}{4} ld(h_n^{-1})).
\end{aligned}
$$

We see that the terms depending only on h_i or h_j with $i, j \neq n$ are cancelled, and just the h_n-terms remain. However, the terms that depend on products of h_i and h_j are accumulated, and this results in an additional $\log(h_n^{-1})$-term.

Altogether, we get an error estimation of the order $O(h_n^2 \log(h_n^{-1}))$ for the combined solution.

The idea of the combination of solutions on different grids can be generalized to three dimensions in a straightforward way. Then, we have three-dimensional grids on the unit cube with the mesh sizes h_i, h_j and h_k in the x-, y- and z-direction. The discrete FE-solutions on a grid $\Omega_{i,j,k}$ will now be denoted by $u_{i,j,k}$.

For a sufficiently smooth solution we assume an expansion of the error on grid $\Omega_{i,j,k}$ like

$$
\begin{aligned}
u - u_{i,j,k} \;&=\; C_1(h_i)h_i^2 \;+\; C_2(h_j)h_j^2 \;+\; C_3(h_k)h_k^2 \\
&+\; D_1(h_i,h_j)h_i^2 h_j^2 \;+\; D_2(h_i,h_k)h_i^2 h_k^2 \;+\; D_3(h_j,h_k)h_j^2 h_k^2 \\
&+\; E(h_i,h_j,h_k)h_i^2 h_j^2 h_k^2,
\end{aligned}
$$

where C_1, C_2, C_3, D_1, D_2, D_3 and E are appropriate functions that are bounded from above by a positive constant κ, i.e. $|C_d(h_i)| \le \kappa$, $|D_d(h_i,h_j)| \le \kappa$, $|E(h_i,h_j,h_k)| \le \kappa$ for $d = 1, 2, 3$ and $\forall h_i, h_j, h_k$.

Then, the appropriate combination of solutions is

$$
\hat{u}^c_{n,n,n} \;:=\; \sum_{i+j+k=n+2} u_{i,j,k} \;-\; 2 \sum_{i+j+k=n+1} u_{i,j,k} \;+\; \sum_{i+j+k=n} u_{i,j,k},
$$

and for the error we get

$$
u - \hat{u}^c_{n,n,n} \;=\; \sum_{i+j+k=n+2} (u - u_{i,j,k}) \;-\; 2 \sum_{i+j+k=n+1} (u - u_{i,j,k}) \;+\; \sum_{i+j+k=n} (u - u_{i,j,k}).
$$

The error expansion leads to the following combination of the different error terms:

$$
\begin{aligned}
& u - \hat{u}^c_{n,n,n} \\
=\; & \sum_{i=1}^{n}(n-i+1)C_1(h_i)h_i^2 \;+\sum_{j=1}^{n}(n-j+1)C_2(h_j)h_j^2 \;+\sum_{k=1}^{n}(n-k+1)C_3(h_k)h_k^2 \\
-\; & 2\left(\sum_{i=1}^{n-1}(n-i)C_1(h_i)h_i^2 \;+\; \sum_{j=1}^{n-1}(n-j)C_2(h_j)h_j^2 \;+\; \sum_{k=1}^{n-1}(n-k)C_3(h_k)h_k^2\right) \\
+\; & \sum_{i=1}^{n-2}(n-i-1)C_1(h_i)h_i^2 \;+\sum_{j=1}^{n-2}(n-j-1)C_2(h_j)h_j^2 \;+\sum_{k=1}^{n-2}(n-k-1)C_3(h_k)h_k^2
\end{aligned}
$$

$$
\begin{aligned}
&+ \sum_{i+j\le n+1} D_1(h_i,h_j)h_i^2h_j^2 + \sum_{i+k\le n+1} D_2(h_i,h_k)h_i^2h_k^2 + \sum_{j+k\le n+1} D_3(h_j,h_k)h_j^2h_k^2 \\
&- 2\left(\sum_{i+j\le n} D_1(h_i,h_j)h_i^2h_j^2 + \sum_{i+k\le n} D_2(h_i,h_k)h_i^2h_k^2 + \sum_{j+k\le n} D_3(h_j,h_k)h_j^2h_k^2\right) \\
&+ \sum_{i+j\le n-1} D_1(h_i,h_j)h_i^2h_j^2 + \sum_{i+k\le n-1} D_2(h_i,h_k)h_i^2h_k^2 + \sum_{j+k\le n-1} D_3(h_j,h_k)h_j^2h_k^2 \\
&+ \sum_{i+j+k=n+2} E(h_i,h_j,h_k)h_i^2h_j^2h_k^2 \\
&- 2\sum_{i+j+k=n+1} E(h_i,h_j,h_k)h_i^2h_j^2h_k^2 \\
&+ \sum_{i+j+k=n} E(h_i,h_j,h_k)h_i^2h_j^2h_k^2.
\end{aligned}
$$

We get this result for the combination of the errors because for example for the first C_1-term it holds that

$$\sum_{i+j+k=n+2} C_1(h_i)h_i^2 = \sum_{i=1}^{n}(n-i+1)C_1(h_i)h_i^2,$$

and for the first D_1-term it holds that

$$\sum_{i+j+k=n+2} D_1(h_i,h_j)h_i^2h_j^2 = \sum_{i+j\le n+1} D_1(h_i,h_j)h_i^2h_j^2$$

as can be seen after a short calculation. Analogous formulas are valid for the other terms.

Now we consider the combination of the different error terms. For the combination of the C_1-terms we get

$$
\begin{aligned}
&\sum_{i=1}^{n}(n-i+1)C_1(h_i)h_i^2 - 2\sum_{i=1}^{n-1}(n-i)C_1(h_i)h_i^2 + \sum_{i=1}^{n-2}(n-i-1)C_1(h_i)h_i^2 \\
&= \sum_{i=1}^{n-2}\Big((n-i+1)-2(n-i)+(n-i-1)\Big)C_1(h_i)h_i^2 \\
&+ \Big((n-(n-1)+1)-2(n-(n-1))\Big)C_1(h_{n-1})h_{n-1}^2 \\
&+ (n-n+1)C_1(h_n)h_n^2 \\
&= C_1(h_n)h_n^2.
\end{aligned}
$$

Analogous formulas are valid for the combination of the C_2- and C_3-terms. We see that the terms depending only on h_i, h_j or h_k with $i,j,k \neq n$ are cancelled like in the two-dimensional case.

For the combination of the D_1-terms we get

$$
\begin{aligned}
&\sum_{i+j\le n+1} D_1(h_i,h_j)h_i^2h_j^2 - 2\sum_{i+j\le n} D_1(h_i,h_j)h_i^2h_j^2 + \sum_{i+j\le n-1} D_1(h_i,h_j)h_i^2h_j^2 \\
&= \sum_{i+j\le n-1}(1-2+1)D_1(h_i,h_j)h_i^2h_j^2
\end{aligned}
$$

$$
\begin{aligned}
&+ \sum_{i+j=n} (1-2) D_1(h_i,h_j) h_i^2 h_j^2 \;+\; \sum_{i+j=n+1} D_1(h_i,h_j) h_i^2 h_j^2 \\
&= \sum_{i+j=n+1} D_1(h_i,h_j) h_i^2 h_j^2 \;-\; \sum_{i+j=n} D_1(h_i,h_j) h_i^2 h_j^2 \\
&= \left(\frac{1}{4} \sum_{i+j=n+1} D_1(h_i,h_j) \;-\; \sum_{i+j=n} D_1(h_i,h_j) \right) \; h_n^2 .
\end{aligned}
$$

Analogous formulas are valid for the combination of the D_2- and D_3-terms. Note that this is just the same result as in the two-dimensional case.

With the previous results and estimations of the type

$$
\begin{aligned}
\Big| \sum_{i+j+k=n+2} E(h_i,h_j,h_k) h_i^2 h_j^2 h_k^2 \Big| \;&\leq\; \sum_{i+j+k=n+2} |E(h_i,h_j,h_k)| \; h_{n+2}^2 \\
&\leq\; \kappa \frac{n(n+1)}{2} h_{n+2}^2
\end{aligned}
$$

that we will need for the combination of the E-terms we get at last

$$
\begin{aligned}
|u - \hat{u}^c_{n,n,n}| \;&\leq\; 3\kappa h_n^2 \\
&+\; 3\kappa h_n^2 (\frac{1}{4} n + n - 1) \\
&+\; \kappa h_n^2 \left(\frac{1}{16} \frac{n(n+1)}{2} \;+\; \frac{2}{4} \frac{(n-1)n}{2} \;+\; \frac{(n-2)(n-1)}{2} \right) \\
&=\; \kappa h_n^2 \left(1 + \frac{65}{32} n \;+\; \frac{25}{32} n^2 \right) \\
&=\; \kappa h_n^2 \left(1 + \frac{65}{32} ld(h_n^{-1}) \;+\; \frac{25}{32} (ld(h_n^{-1}))^2 \right) .
\end{aligned}
$$

Altogether, we see that in the three-dimensional case we have an error bound of the order $O(h_n^2 \; (\log(h_n^{-1}))^2)$. Note that this type of proof easily extends to higher dimensions.

To some extent this argumentation might even hold for problems with non-smooth solutions and higher order discretization methods. But there, we would need a more refined theory of asymptotic error expansions. At least, the results of the following numerical experiments are promising.

4. Numerical Experiments. To demonstrate the advantages of our combination approach let us consider a couple of two-dimensional model problems. The results for model problems 1 to 3 have been computed in double precision on a DECstation2100 with 16 megabyte storage. The results for the model problems 4 and 5 have been computed in single precision on an Apollo DN 4500 using the NISA II finite element package.

We want to compare the quality of the solution that was obtained for the standard full grid to the quality of the solution that was created by the combination approach. Therefore, for the combination approach we consider the projected error $e^c_{n,n} := \hat{u}^c_{n,n} - u^I_{n,n}$ on grid $\Omega_{n,n}$, where $u^I_{n,n}$ is the interpolant of the exact solution into $S^0_{n,n}$. Thus, we interpolate the solution $\hat{u}^c_{n,n}$ that is obtained by the combination approach from the sparse grid space $\hat{S}^0_{n,n}$ to the full grid space $S^0_{n,n}$ and subtract here the interpolant of the exact solution u. For the usual full grid method with the solution $u_{n,n}$ we consider the error $e_{n,n} := u_{n,n} - u^I_{n,n}$ on grid $\Omega_{n,n}$.

The discrete L_2-norm is defined using only the interior grid points, i.e.

$$\|e_{n,n}\|_2 \;=\; \frac{\sqrt{e^T_{n,n}e_{n,n}}}{2^n - 1}.$$

The discrete L_∞-norm is defined as usual by

$$\|e_{n,n}\|_\infty \;=\; max|e_{n,n}(x,y)|.$$

4.1. Problem 1: (Smooth solution). The first problem is

$$\Delta u \;=\; 0 \qquad \text{in} \;\; \Omega$$

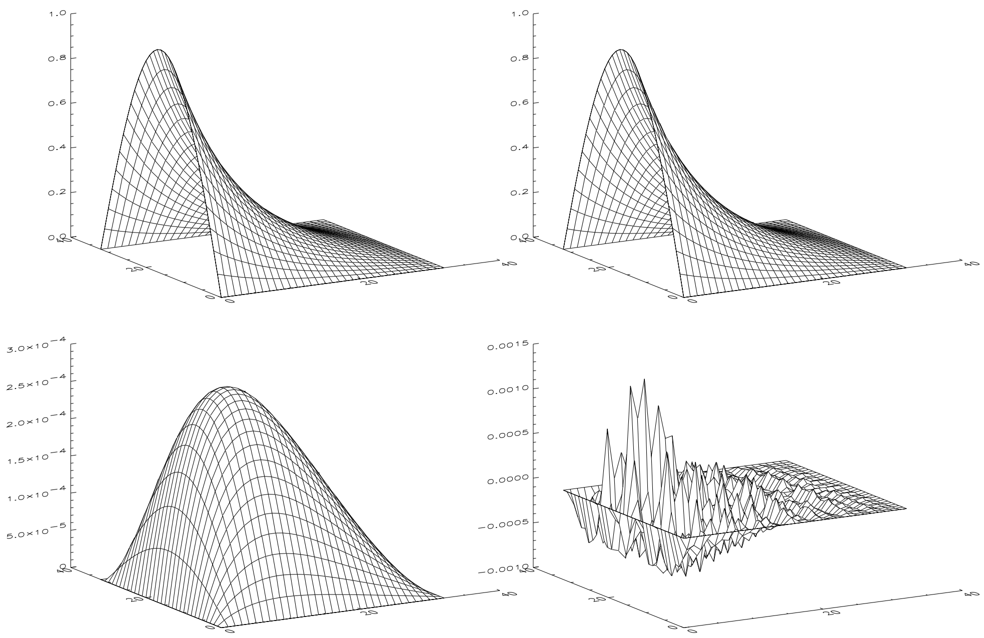

FIG. 4. $u_{5,5}$ *and* $e_{5,5}$ *(on the left),* $u^c_{5,5}$ *and* $e^c_{5,5}$ *(on the right) for model problem 1.*

with the exact solution

$$u \;=\; \sin(\pi y)\frac{\sinh(\pi(1-x))}{\sinh(\pi)}$$

and Dirichlet boundary conditions on $\delta\Omega$.

We see in figure 4 that the error of the solution $u_{n,n}$ that was computed on the full grid $\Omega_{n,n}$ and the error that was obtained by the new combination technique are of different types. In the first case the error is smooth while in the second case it is oscillating. Note that the error of the combined solution is for the L_2-norm about the factor 1.5 and for the L_∞-norm about the factor 5 worse. The errors in figure 4 are not equally scaled.

TABLE 1

Pointwise error, full grid on the left, combined solution on the right.

n	$e_{n,n}(\frac{1}{2},\frac{1}{2})$	$\frac{\lvert e_{n-1,n-1}\rvert}{\lvert e_{n,n}\rvert}$	$e_{n,n}(\frac{1}{4},\frac{1}{4})$	$\frac{\lvert e_{n-1,n-1}\rvert}{\lvert e_{n,n}\rvert}$	$e^c_{n,n}(\frac{1}{2},\frac{1}{2})$	$\frac{\lvert e^c_{n-1,n-1}\rvert}{\lvert e^c_{n,n}\rvert}$	$e^c_{n,n}(\frac{1}{4},\frac{1}{4})$	$\frac{\lvert e^c_{n-1,n-1}\rvert}{\lvert e^c_{n,n}\rvert}$
1	7.4268E-2	-	-	-	7.4268E-2	-	-	-
2	1.5498E-2	4.792	1.3252E-2	-	9.9913E-3	7.433	-9.3480E-3	-
3	3.7333E-3	4.151	3.1526E-3	4.204	1.2929E-3	7.727	6.1846E-3	1.511
4	9.2504E-4	4.036	7.7889E-4	4.048	5.5787E-5	23.176	1.2064E-3	5.126
5	2.3075E-4	4.009	1.9415E-4	4.012	-5.1448E-5	1.084	2.2655E-4	5.325
6	5.7655E-5	4.002	4.8503E-5	4.003	-2.9150E-5	1.764	3.8414E-5	5.897
7	1.4412E-5	4.001	1.2123E-5	4.001	-1.1357E-5	2.566	5.0772E-6	7.566
8	3.6028E-6	4.000	3.0307E-6	4.000	-3.8568E-6	2.944	1.3935E-7	3.643
9	9.0070E-7	4.000	7.5768E-7	4.000	-1.2186E-6	3.165	-2.4756E-7	0.562
10	2.2517E-7	4.000	1.8942E-7	4.000	-3.6824E-7	3.309	-1.3249E-7	1.868
11					-1.0796E-7	3.410	-5.0770E-8	2.609
12					-3.0964E-8	3.486	-1.7105E-8	2.968
13					-8.7346E-9	3.544	-5.3792E-9	3.179

Table 1 shows the pointwise behaviour of the error of the solution that was achieved on the full grid and by the new combination technique. We consider here only the points P1=(0.5,0.5) and P2=(0.25,0.25).

Table 2 shows the behaviour of the L_2- and L_∞-norm of the errors.

TABLE 2

L_2- and L_∞-norm of the error, full grid on the left, combined solution on the right.

n	$\lvert e_{n,n}\rvert_2$	$\frac{\lvert e_{n-1,n-1}\rvert_2}{\lvert e_{n,n}\rvert_2}$	$\lvert e_{n,n}\rvert_\infty$	$\frac{\lvert e_{n-1,n-1}\rvert_\infty}{\lvert e_{n,n}\rvert_\infty}$	$\lvert e^c_{n,n}\rvert_2$	$\frac{\lvert e^c_{n-1,n-1}\rvert_2}{\lvert e^c_{n,n}\rvert_2}$	$\lvert e^c_{n,n}\rvert_\infty$	$\frac{\lvert e^c_{n-1,n-1}\rvert_\infty}{\lvert e^c_{n,n}\rvert_\infty}$
1	7.4268E-2	-	7.4268E-2	-	7.4268E-2	-	7.4268E-2	-
2	1.2047E-2	6.165	1.8742E-2	3.963	1.4123E-2	5.258	3.2387E-2	2.293
3	2.5072E-3	4.805	4.4585E-3	4.204	3.2023E-3	4.410	1.2887E-2	2.513
4	5.7950E-4	4.326	1.1169E-3	3.992	7.9926E-4	4.007	4.5351E-3	2.841
5	1.3985E-4	4.144	2.7847E-4	4.011	2.1322E-4	3.748	1.4838E-3	3.056
6	3.4385E-5	4.067	6.9659E-5	3.998	5.9058E-5	3.610	5.0056E-4	2.964
7	8.5272E-6	4.032	1.7412E-5	4.001	1.6610E-5	3.556	1.5518E-4	3.226
8	2.1234E-6	4.016	4.3528E-6	4.001	4.6816E-6	3.548	4.6647E-5	3.327
9	5.2980E-7	4.008	1.0882E-6	4.000	1.3141E-6	3.563	1.366E7-5	3.413
10	1.3232E-7	4.004	2.7205E-7	4.000	3.6642E-7	3.586	3.9669E-6	3.445

For a smooth solution on a regular full grid we know from the theory that the convergence rate of the discretization error is of the order $O(h^2)$. See i.e. [4]. This is reflected in the left part of table 1 and 2. Here a limit value of 4.0 for the quotient $|e_{n-1,n-1}|/|e_{n,n}|$ can be seen for all norms.

For the solution that was obtained by the combination technique we proved a discretization error of the order $O(h^2\log(h^{-1}))$. The influence of the log-term can be seen in the right part of table 1 and 2.

Despite of that, the error is of nearly the same size as the error on the associated full grid. But remember that the number of grid points and thus the number of floating point operations that are necessary to solve the different problems i.e. by a multigrid method is of order $O(h_n^{-2})$ for the full grid and only of order $O(h_n^{-1}\log(h_n^{-1}))$ for the combination technique.

For our model problem with a smooth solution we have seen that the new combination technique behaves superior to the standard grid approach. The following experiments show that this is also true for more complicated problems.

4.2. Problem 2: (Singular solution). The second problem is

$$\Delta u \;=\; 0 \qquad \text{in } \; \Omega = [0,1]\times[-0.5,0.5]$$

with the solution

$$u \;=\; RE(z^{\frac{1}{2}}) \;=\; (x^2+y^2)^{\frac{1}{4}} \cos\Big(\frac{\arctan(\frac{x}{y})}{2}\Big)$$

and Dirichlet boundary conditions on $\delta\Omega$. The solution has a singularity in (0,0).

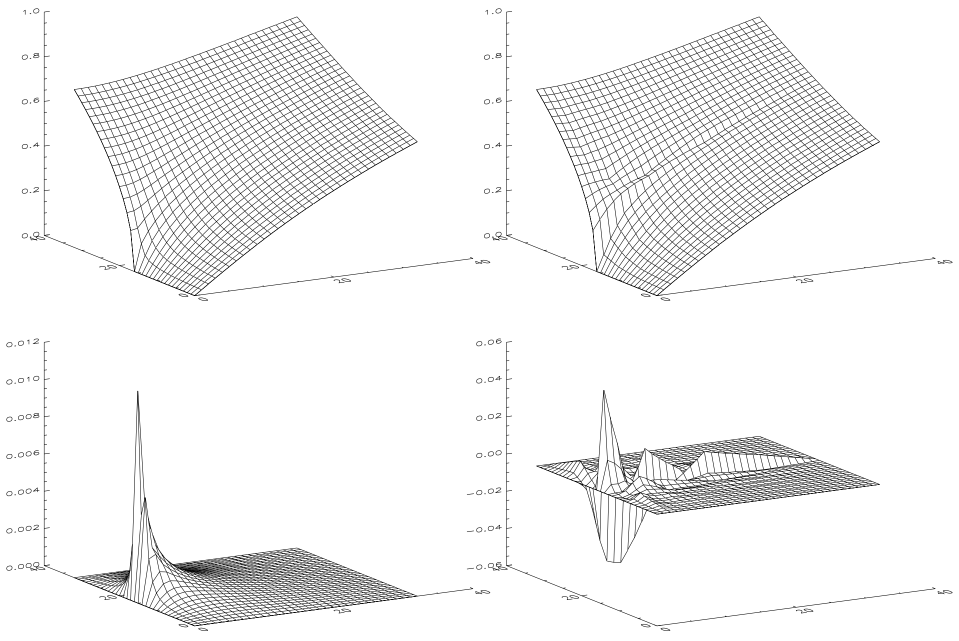

FIG. 5. *$u_{5,5}$ and $e_{5,5}$ (on the left), $u^c_{5,5}$ and $e^c_{5,5}$ (on the right) for model problem 2.*

Once more we see the different behaviour of the error for the solution computed on the full grid $\Omega_{n,n}$ and the error that was obtained by the new combination technique. The error on the full grid is smooth but the error for the combined solution is oscillating.

Additionally, the singularity leads to a different pollution effect. In the case of the full grid the pollution spreads radially and declines logarithmically with the distance from the singularity. For the combination-error, however, the pollution is spread due to the product-type interpolation crosswise in the x- and y-direction. In our example where the singularity is situated at the boundary of the domain the polluted area is T-shaped, as can be seen from figure 5. The error parallel to the grid line $x = 0$, however, is relatively small.

Table 3 shows the pointwise behaviour of the error of the solution that was achieved on the full grid $\Omega_{n,n}$ and by the new combination technique. We consider here the points P1=(0.5,0.0) and P2=(0.25,-0.25).

Table 4 shows the behaviour of the L_2- and L_∞-norm of the error.

From the theory we know that for the full grid a pointwise convergence rate of $O(h^{3/2})$ can be expected in a sufficient distance away from the singularity. Near the singularity, however, only a convergence rate of $O(h^{1/2})$ can be achieved. See [4]. This is seen in the left part of table 3 and 4. For the pointwise norms a quotient of $2^{3/2} \approx 2.828$ and for the L_∞-norm a quotient of $2^{1/2} \approx 1.414$ will be reached in the limit.

TABLE 3
Pointwise error, full grid on the left, combined solution on the right.

n	$e_{n,n}(\frac{1}{2},0)$	$\frac{\lvert e_{n-1,n-1}\rvert}{\lvert e_{n,n}\rvert}$	$e_{n,n}(\frac{1}{4},-\frac{1}{4})$	$\frac{\lvert e_{n-1,n-1}\rvert}{\lvert e_{n,n}\rvert}$	$e^c_{n,n}(\frac{1}{2},0)$	$\frac{\lvert e^c_{n-1,n-1}\rvert}{\lvert e^c_{n,n}\rvert}$	$e^c_{n,n}(\frac{1}{4},-\frac{1}{4})$	$\frac{\lvert e^c_{n-1,n-1}\rvert}{\lvert e^c_{n,n}\rvert}$
1	3.9695E-3	-	-	-	3.9695E-3	-	-	-
2	6.3484E-3	0.625	1.2359E-2	-	-7.5628E-3	0.5248	-1.4178E-3	-
3	2.7436E-3	2.314	3.9539E-3	3.126	-3.4260E-3	2.2075	1.1336E-2	0.125
4	1.0995E-3	2.495	1.3877E-3	2.849	5.7404E-4	5.9681	1.3736E-3	8.253
5	4.1708E-4	2.674	5.0905E-4	2.726	1.2047E-3	0.4765	7.4114E-4	1.853
6	1.5408E-4	2.707	1.8525E-4	2.748	7.6178E-4	1.5814	-2.2430E-6	330.429
7	5.6081E-5	2.747	6.6799E-5	2.773	4.1336E-4	1.8429	4.5173E-6	0.497
8	2.0225E-5	2.773	2.3929E-5	2.792	1.8820E-4	2.1964	-5.4202E-6	0.833
9	7.2498E-6	2.789	8.5351E-6	2.804	7.7368E-5	2.4325	-3.1142E-6	1.741
10	2.5879E-6	2.801	3.0357E-6	2.812	3.0123E-5	2.5684	-1.4430E-6	2.158
11					1.1331E-5	2.6585	-5.9843E-7	2.411
12					4.1710E-6	2.7165	-2.3432E-7	2.554
13					1.5146E-6	2.7538	-8.8687E-8	2.642
14					5.4518E-7	2.7781	-3.2851E-8	2.700
15					1.9512E-7	2.7940	-1.1997E-8	2.738

TABLE 4
L_2- and L_∞-norm of the error, full grid on the left, combined solution on the right.

n	$\lvert e_{n,n}\rvert_2$	$\frac{\lvert e_{n-1,n-1}\rvert_2}{\lvert e_{n,n}\rvert_2}$	$\lvert e_{n,n}\rvert_\infty$	$\frac{\lvert e_{n-1,n-1}\rvert_\infty}{\lvert e_{n,n}\rvert_\infty}$	$\lvert e^c_{n,n}\rvert_2$	$\frac{\lvert e^c_{n-1,n-1}\rvert_2}{\lvert e^c_{n,n}\rvert_2}$	$\lvert e^c_{n,n}\rvert_\infty$	$\frac{\lvert e^c_{n-1,n-1}\rvert_\infty}{\lvert e^c_{n,n}\rvert_\infty}$
1	3.9695E-3	-	3.9695E-3	-	3.9695E-3	-	3.9695E-3	-
2	1.1000E-2	0.361	2.7093E-2	0.147	1.9356E-2	0.205	3.6331E-2	0.109
3	4.6957E-3	2.343	2.1732E-2	1.247	1.2190E-2	1.588	5.3937E-2	0.674
4	1.9065E-3	2.463	1.5744E-2	1.380	7.5137E-3	1.622	5.7539E-2	0.937
5	7.5691E-4	2.519	1.1195E-2	1.406	4.6105E-3	1.629	5.3173E-2	1.082
6	2.9572E-4	2.559	7.9270E-3	1.413	2.8254E-3	1.632	4.5382E-2	1.172
7	1.1405E-4	2.593	5.6071E-3	1.414	1.7246E-3	1.638	3.7325E-2	1.216
8	4.3523E-5	2.621	3.9651E-3	1.414	1.0491E-3	1.644	3.1997E-2	1.167
9	1.6463E-5	2.644	2.8038E-3	1.414	6.3508E-4	1.652	2.6971E-2	1.186
10	6.1820E-6	2.663	1.9826E-3	1.414	3.8318E-4	1.657	2.2621E-2	1.192

In the case of a non-smooth solution the theory for the combination technique is still not complete. However, the results of the numerical experiments of the right part of table 3 and 4 indicate that there might be only an additional $\log(h^{-1})$-factor just like in the case of a smooth solution. Disturbed by such a $\log(h^{-1})$-factor the pointwise error might still tend to a quotient of 2.828 and in the L_∞-norm to a quotient of 1.414. But this can not be seen clearly.

The behaviour of the L_2-norm reflects the difference of the size and shape of the polluted area. Due to the interpolation, the polluted area is much larger for the combination technique and has a different shape. Here, further studies are necessary.

4.3. Problem 3: (Boundary layer). We consider now the convection diffusion problem

$$\epsilon\Delta u \;+\; u_x \;=\; f \qquad \text{in } \Omega$$

with the exact solution

$$u \;=\; \Big(\exp(\frac{-x}{\epsilon}) - \exp(\frac{-1}{\epsilon})\Big) \;/\; \Big(1-\exp(\frac{-1}{\epsilon})\Big),$$

Dirichlet boundary conditions for $y=0$, $y=1$ and the Neumann boundary conditions $u_n = 0$ for $x=0$, $x=1$. This problem has an exponential boundary layer near the downstream boundary. Note that the solution depends only on x.

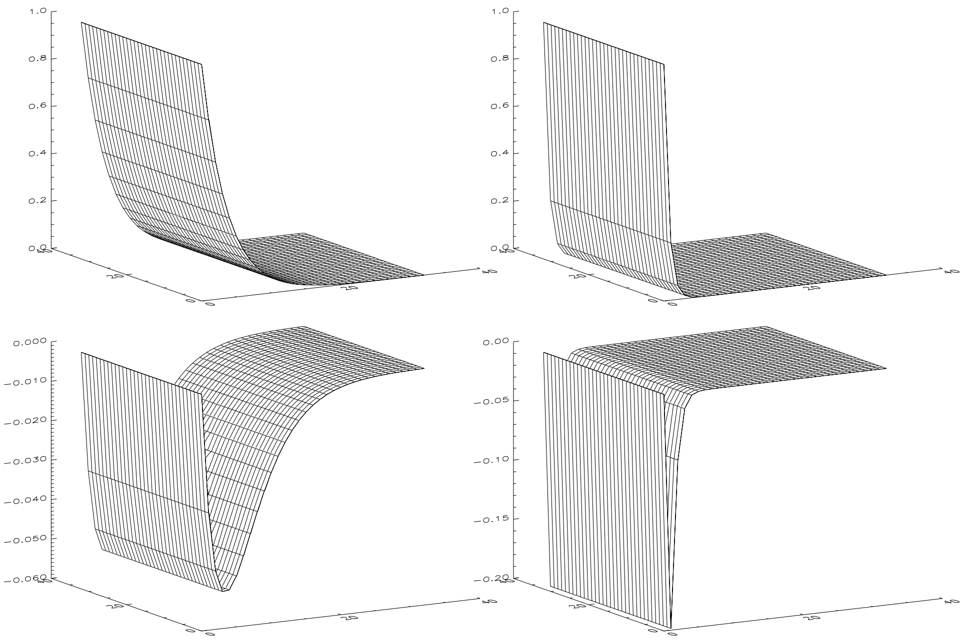

FIG. 6. *$u^c_{5,5}$ and $e^c_{5,5}$ for $\epsilon = 0.1$ and $\epsilon = 0.01$ for problem 3.*

As we have to compute solutions on extremely distorted grids $\Omega_{i,j}$ with $i \gg j$ or $i \ll j$, we have to face the problem of instable discretizations for central differences. To prevent this we used upwind differences instead.

For this special model problem our combination technique gives a solution $\hat{u}^c_{n,n}$ which is **equal** to the solution that is obtained on the full grid $\Omega_{n,n}$. In general, solutions that depend only on x or y and boundary layers parallel to the x- or y-axis are very well resolved by the combination technique. However, for problems with strong convection in the diagonal direction, this is not true.

Table 5 shows the behaviour of the error for moderate convection with $\epsilon = 0.1$.

TABLE 5

Pointwise error, L_2- and L_∞-norm of the error for $\epsilon = 0.1$.

n	$e^c_{n,n}(\frac{1}{2},\frac{1}{2})$	$\frac{\lvert e^c_{n-1,n-1}\rvert}{\lvert e^c_{n,n}\rvert}$	$e^c_{n,n}(\frac{1}{4},\frac{1}{4})$	$\frac{\lvert e^c_{n-1,n-1}\rvert}{\lvert e^c_{n,n}\rvert}$	$\lvert e^c_{n,n}\rvert_2$	$\frac{\lvert e^c_{n-1,n-1}\rvert_2}{\lvert e^c_{n,n}\rvert_2}$	$\lvert e^c_{n,n}\rvert_\infty$	$\frac{\lvert e^c_{n-1,n-1}\rvert_\infty}{\lvert e^c_{n,n}\rvert_\infty}$
1	-1.3616E-1	-	-	-	1.3616E-1	-	1.3616E-1	-
2	-6.8779E-2	1.980	-1.9888E-1	-	1.2186E-1	1.117	1.9888E-1	0.685
3	-3.0860E-2	2.229	-1.1426E-1	1.741	7.8273E-2	1.557	1.5713E-1	1.266
4	-1.3460E-2	2.293	-6.1007E-2	1.873	4.3562E-2	1.797	9.1963E-2	1.709
5	-6.0377E-3	2.229	-3.1364E-2	1.945	2.3055E-2	1.889	5.0614E-2	1.817
6	-2.8174E-3	2.143	-1.5861E-2	1.977	1.1902E-2	1.937	2.6954E-2	1.878
7	-1.3547E-3	2.080	-7.9685E-3	1.991	6.0552E-3	1.966	1.3910E-2	1.938
8	-6.6344E-4	2.042	-3.9926E-3	1.996	3.0553E-3	1.982	7.0650E-3	1.969
9	-8.9658E-5	7.399	-1.8728E-3	2.132	1.4790E-3	2.066	3.5068E-3	2.015

Table 6 shows the behaviour of the error for $\epsilon = 0.01$.

We used upwind differences and, as mentioned before, we get the same solution by the combination technique as for the standard grid approach. Therefore, we can expect a convergence rate of $O(h)$ and an error quotient of 2 if the boundary layer is sufficiently resolved. This can be seen clearly in table 5. In the case of $\epsilon = 0.01$ a finer

TABLE 6
Pointwise error, L_2- and L_∞-norm of the error for $\epsilon = 0.01$.

n	$e^c_{n,n}(\frac{1}{2},\frac{1}{2})$	$\frac{\lvert e^c_{n-1,n-1}\rvert}{\lvert e^c_{n,n}\rvert}$	$e^c_{n,n}(\frac{1}{4},\frac{1}{4})$	$\frac{\lvert e^c_{n-1,n-1}\rvert}{\lvert e^c_{n,n}\rvert}$	$\lvert e^c_{n,n}\rvert_2$	$\frac{\lvert e^c_{n-1,n-1}\rvert_2}{\lvert e^c_{n,n}\rvert_2}$	$\lvert e^c_{n,n}\rvert_\infty$	$\frac{\lvert e^c_{n-1,n-1}\rvert_\infty}{\lvert e^c_{n,n}\rvert_\infty}$
1	-1.9231E-02	-	-	-	1.9231E-2	-	1.9231E-2	-
2	-1.4771E-03	13.019	-3.8459E-02	-	2.2221E-2	0.865	3.8459E-2	0.500
3	-3.0106E-05	49.064	-5.4869E-03	7.009	2.8073E-2	0.792	7.4070E-2	0.519
4	-1.3101E-07	229.799	-3.6195E-04	15.159	3.5464E-2	0.792	1.3600E-1	0.545
5	-1.4230E-10	920.660	-1.1929E-05	30.342	3.7175E-2	0.954	1.9849E-1	0.685
6	-8.3100E-14	1712.395	-2.8931E-07	41.236	2.7439E-2	1.355	1.8063E-1	1.099
7	0.0	-	-9.4660E-09	30.567	1.6248E-2	1.689	1.0556E-1	1.711
8	0.0	-	-6.6932E-10	14.143	8.8439E-3	1.837	6.2066E-2	1.701
9	0.0	-	-1.0697E-10	6.257	4.6337E-3	1.909	3.3216E-2	1.859

grid is needed for the resolution of the boundary layer. But then the error quotient of 2 will be reached as can be seen in table 6.

4.4. Problem 4: (Distorted quadrilateral and triangular elements). The new combination technique works not only for problems on the unit square but also in the general case of distorted quadrilateral elements and especially for triangular elements. To show this, we consider the model problem

$$\Delta u \;=\; 0 \qquad \text{in } \; \Omega_\alpha$$

with the exact solution

$$u \;=\; \sin\Big(\pi(\frac{1}{2}x + \frac{1}{2}\sqrt{3}y)\Big)\; \sinh\Big(\pi(1 - \frac{1}{2}\sqrt{3}x + \frac{1}{2}y)\Big) / \sinh(\pi)$$

and Dirichlet boundary conditions.

Here, we rotated the function u of problem 1 using the matrix

$$\begin{pmatrix} \cos\psi & -\sin\psi \\ \sin\psi & \cos\psi \end{pmatrix}$$

by $\psi = 30^0$ counterclockwise to avoid the special situation that the symmetry-axis of the solution u is parallel to the x-axis.

The distorsion of the domain Ω_α is described by the parameter α. This is shown in figure 7.

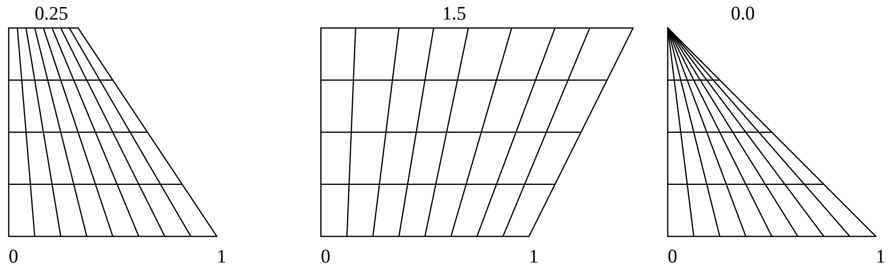

FIG. 7. *Distorted domains and grids for different values of α.*

For $\alpha = 1$ we get the unit square, and for $\alpha > 1$ we get an overstretched quadrilateral with an interior angle at (1,0) larger than 90^0. For $\alpha < 1$ we get a contracted quadrilateral with an interior angle at (1,0) smaller than 90^0.

For $\alpha = 0$ we get a triangle with the corner points (0,0), (0,1) and (1,0). The grid lines in y-direction intersect now in the point (0,1). Note that the grids over this domain contain now quadrilateral and triangular elements.

For the solution of the different problems arising in the combination approach we used the NISA II finite element package.

The L_2- and L_∞-norms of the error for the triangular domain with $\alpha = 0$ are shown in table 7.

TABLE 7
L_2- and L_∞-norm of the error, $\alpha = 0$, full grid on the left, combined solution on the right.

n	$\vert e_{n,n}\vert_2$	$\frac{\vert e_{n-1,n-1}\vert_2}{\vert e_{n,n}\vert_2}$	$\vert e_{n,n}\vert_\infty$	$\frac{\vert e_{n-1,n-1}\vert_\infty}{\vert e_{n,n}\vert_\infty}$	$\vert e^c_{n,n}\vert_2$	$\frac{\vert e^c_{n-1,n-1}\vert_2}{\vert e^c_{n,n}\vert_2}$	$\vert e^c_{n,n}\vert_\infty$	$\frac{\vert e^c_{n-1,n-1}\vert_\infty}{\vert e^c_{n,n}\vert_\infty}$
1	9.5096E-3	-	9.5096E-3	-	9.5096E-3	-	9.5096E-3	-
2	1.1930E-2	0.797	2.1574E-2	0.441	2.3100E-2	0.412	3.8826E-2	2.449
3	4.1537E-3	2.872	1.2797E-2	1.686	6.4787E-3	3.566	1.6726E-3	2.321
4	1.0681E-3	3.889	4.9469E-3	2.587	1.9097E-3	3.392	6.6757E-3	2.505
5	2.5229E-4	4.233	1.5213E-3	3.252	5.6656E-4	3.371	2.4531E-3	2.721
6					1.6662E-4	3.400	8.0565E-4	3.045
7					4.8350E-5	3.446	2.4851E-4	3.242
8					1.3820E-5	3.498	7.5632E-5	3.286
9					3.9029E-6	3.541	2.2351E-5	3.384

The L_2- and L_∞-error-norms for the distorted quadrilateral domain with $0 < \alpha \leq 1$ are shown in table 8.

TABLE 8
L_2- and L_∞-norm of the error, full grid on the left, combined solution on the right.

n	$\vert e_{n,n}\vert_2$	$\frac{\vert e_{n-1,n-1}\vert_2}{\vert e_{n,n}\vert_2}$	$\vert e_{n,n}\vert_\infty$	$\frac{\vert e_{n-1,n-1}\vert_\infty}{\vert e_{n,n}\vert_\infty}$	$\vert e^c_{n,n}\vert_2$	$\frac{\vert e^c_{n-1,n-1}\vert_2}{\vert e^c_{n,n}\vert_2}$	$\vert e^c_{n,n}\vert_\infty$	$\frac{\vert e^c_{n-1,n-1}\vert_\infty}{\vert e^c_{n,n}\vert_\infty}$
	$\alpha = 0.25$							
3	4.2452E-3	4.694	8.4283E-3	3.985	6.4226E-3	3.814	2.1837E-2	2.390
4	9.8476E-4	4.311	2.0835E-3	4.045	1.7699E-3	3.629	7.3578E-3	2.968
5	2.3782E-4	4.141	5.1973E-4	4.009	5.0109E-4	3.533	2.4429E-3	3.012
6					1.4269E-4	3.511	7.6540E-4	3.192
7					4.0502E-5	3.523	2.3221E-4	3.296
8					1.1407E-5	3.551	6.9677E-5	3.333
9					3.1858E-6	3.580	2.0421E-5	3.412
	$\alpha = 0.50$							
3	3.0432E-3	4.779	6.2919E-3	4.188	5.8794E-3	3.727	1.5760E-2	2.469
4	7.0189E-4	4.336	1.5542E-3	4.048	1.6057E-3	3.662	6.1470E-3	2.564
5	1.6925E-4	4.147	3.8855E-4	3.999	4.4705E-4	3.592	2.1065E-3	2.918
6					1.2559E-4	3.559	6.6544E-4	3.166
7					3.5303E-5	3.558	2.1839E-4	3.047
8					9.8857E-6	3.571	6.6934E-5	3.263
9					2.7416E-6	3.606	1.9953E-5	3.355
	$\alpha = 0.75$							
3	2.1171E-3	4.799	4.3940E-3	4.374	6.0933E-3	3.529	1.7227E-2	2.447
4	4.8576E-4	4.358	1.1166E-3	3.935	1.6843E-3	3.618	5.8312E-3	2.954
5	1.1695E-4	4.154	2.7761E-4	4.022	4.6781E-4	3.600	1.7615E-3	3.310
6					1.3039E-4	3.586	6.0018E-4	2.935
7					3.6314E-5	3.591	1.7619E-4	3.406
8					1.0072E-5	3.606	5.3778E-5	3.276
9					2.7796E-6	3.623	1.6094E-5	3.341
	$\alpha = 1.00$							
3	2.3511E-3	4.684	4.0648E-3	4.169	7.6947E-3	3.441	2.2687E-2	2.073
4	5.4137E-4	4.343	1.0618E-3	3.828	2.1410E-3	3.594	8.1892E-3	2.770
5	1.3042E-4	4.151	2.6508E-4	4.005	5.9493E-4	3.599	2.7016E-3	3.031
6					1.6531E-4	3.599	8.6480E-4	3.124
7					4.5809E-5	3.609	2.7041E-4	3.198
8					1.2634E-5	3.626	8.4791E-5	3.189
9					3.4665E-6	3.645	2.5165E-5	3.369

The L_2- and L_∞-error-norms for the distorted quadrilateral domain with $\alpha > 1$

are shown in table 9.

TABLE 9
L_2- and L_∞-norm of the error, full grid on the left, combined solution on the right.

n	$\lvert e_{n,n}\rvert_2$	$\frac{\lvert e_{n-1,n-1}\rvert_2}{\lvert e_{n,n}\rvert_2}$	$\lvert e_{n,n}\rvert_\infty$	$\frac{\lvert e_{n-1,n-1}\rvert_\infty}{\lvert e_{n,n}\rvert_\infty}$	$\lvert e^c_{n,n}\rvert_2$	$\frac{\lvert e^c_{n-1,n-1}\rvert_2}{\lvert e^c_{n,n}\rvert_2}$	$\lvert e^c_{n,n}\rvert_\infty$	$\frac{\lvert e^c_{n-1,n-1}\rvert_\infty}{\lvert e^c_{n,n}\rvert_\infty}$
	$\alpha = 1.25$							
3	3.1066E-3	4.610	5.7577E-3	4.397	1.0412E-2	3.302	2.8915E-2	1.934
4	7.1723E-4	4.331	1.5199E-3	3.788	2.9519E-3	3.527	1.2425E-2	2.327
5	1.7288E-4	4.149	3.7829E-4	4.018	8.2847E-4	3.563	4.0957E-3	3.033
6					2.3155E-4	3.578	1.2902E-3	3.174
7					6.4408E-5	3.595	4.1142E-4	3.136
8					1.7806E-5	3.617	1.2659E-4	3.250
9					4.8899E-6	3.641	3.8437E-5	3.294
	$\alpha = 1.5$							
3	3.9966E-3	4.597	8.4197E-3	4.079	1.4071E-2	3.163	3.9781E-2	2.173
4	9.2127E-4	4.338	2.1737E-3	3.874	4.0907E-3	3.439	1.8165E-2	2.190
5	2.2192E-4	4.151	5.3943E-4	4.029	1.1634E-3	3.516	6.0234E-3	3.016
6					3.2786E-4	3.548	2.0591E-3	2.925
7					9.1733E-5	3.574	6.6859E-4	3.079
8					2.5477E-5	3.601	2.0600E-4	3.246
9					7.0191E-6	3.629	6.2267E-5	3.308
	$\alpha = 2.0$							
3	6.1333E-3	4.761	1.5431E-2	3.828	2.3703E-2	3.088	7.1046E-2	2.373
4	1.3915E-3	4.408	3.7287E-3	4.138	7.1985E-3	3.293	3.2821E-2	2.165
5	3.3353E-3	4.172	9.3582E-4	3.984	2.0972E-3	3.432	1.1332E-2	2.896
6					5.9997E-4	3.496	3.7535E-3	3.019
7					1.6969E-4	3.536	1.2758E-3	2.942
8					4.7529E-5	3.571	3.9598E-4	3.222
9					1.3192E-5	3.603	1.1923E-4	3.321
	$\alpha = 3.0$							
3	1.3176E-2	5.113	3.8123E-2	3.800	5.4262E-2	2.917	1.5924E-1	2.062
4	2.8313E-3	4.654	8.5733E-3	4.447	1.8186E-2	2.984	6.6950E-2	2.378
5	6.6666E-4	4.247	2.0848E-3	4.112	5.9658E-3	3.048	2.3757E-2	2.818
6					1.9597E-3	3.044	8.4016E-3	2.828
7					6.3069E-4	3.107	3.0049E-3	2.796
8					1.9663E-4	3.207	9.7284E-4	3.089
9					5.9446E-5	3.308	3.1372E-4	3.101
	$\alpha = 5.0$							
3	1.9070E+0	3.579	1.0963E+1	1.855	2.3518E+1	1.255	1.1007E+2	0.749
4	4.3402E-1	4.394	2.6535E+0	4.132	1.0950E+1	2.148	6.2188E+1	1.770
5	1.0337E-1	4.198	7.3034E-1	3.633	4.3281E+0	2.530	3.0049E+1	2.070
6					1.5618E+0	2.771	1.2018E+1	2.500
7					5.3668E-1	2.910	4.4339E+0	2.710
8					1.7765E-1	3.021	1.5944E+0	2.781
9					5.6619E-2	3.138	5.2913E-1	3.013

The combination technique shows for triangles and moderately distorted quadrilateral domains ($0.25 \leq \alpha < 3$) practically the same good results and error quotients as for the unit square. This includes even the triangular case with $\alpha = 0$. Only for the quadrilateral domains with $\alpha = 3$ or 5 the results are not yet fully satisfying. But the error quotient improves for rising n. Therefore, we expect that for a sufficiently large n the combination technique is still more efficient than the full grid approach.

Here, we only listed the results for the L_2 and L_∞-norms of the error. The pointwise error behaves nearly the same. By restrictions of the version of the FE-package we used, the tables are incomplete.

But the results show once more the superiority of the new technique, especially when storage aspects have to be taken into account.

These experiments give us an idea how a problem with general polygonal boundary can be treated. First, a coarse mesh consisting of triangular and moderately distorted quadrilateral elements that resolves the boundary sufficiently has to be designed. Then, on every such element the grids $\Omega^e_{i,j}$, $i+j = n, n+1$, can be constructed.

The union of the element grids results in the meshes $\Omega_{i,j}$ on the whole domain. Now, we solve the associated problems $P_{i,j}$, and combine the solutions according to chapter 3.

4.5. Problem 5: (Nonlinear heat transfer). The combination technique might also be used for nonlinear problems. To show an example we consider the nonlinear heat transfer problem

$$\frac{\partial}{\partial x}\left(\epsilon_\alpha(u)\frac{\partial u}{\partial x}\right) \;+\; \frac{\partial}{\partial y}\left(\epsilon_\alpha(u)\frac{\partial u}{\partial y}\right) \;=\; f \quad \text{in } \Omega$$

with the exact solution

$$u \;=\; \sin(\pi y)\frac{\sinh(\pi(1-x))}{\sinh(\pi)}$$

and Dirichlet boundary conditions on $\delta\Omega$. The material property function is

$$\epsilon_\alpha(u) \;=\; \begin{cases} 1-(u-1/2)^{1/\alpha} & u > 1/2 \\ 1 & u = 1/2 \\ 1+(1/2-u)^{1/\alpha} & u < 1/2. \end{cases}$$

For the combined solution we solved the arising **nonlinear** problems $L_{i,j}u_{i,j} \;=\; f_{i,j}$, $i+j=n, n+1$, using the NISA II finite element package.

Table 10 shows the behaviour of the L_2- and L_∞-norm of the error.

By restrictions of the version of the FE-package we used, the tables are incomplete.

Note that the solution of any of the problems $P_{i,j}$, $i+j=n, n+1$, can serve as a very good start value for the other problems, reducing the execution time of the Newton iteration substantially.

We see in table 10 that the combination technique produces good solutions even in the nonlinear case. Here, the error quotient is not as large as in the previous experiments. But for all regarded values of α the error quotient is increasing for rising n. Therefore, we expect for sufficiently large values of n even in the nonlinear case a similar convergence behaviour of the combination technique as in the linear case.

If we regard the efficiency comparing the degrees of freedom, the run time and the achieved accuracy, the combination technique is superior to the full grid approach already for small values of n.

For large values of α the combination approach might loose this superiority. Additional outer Newton iterations seem to be a remedy. Here further studies are necessary.

5. Concluding Remarks. We have seen that in many situations the combination technique leads to the cancellation of certain error terms in the asymptotic error expansion. Altogether, in the two-dimensional case an accuracy of $O(h_n^2 \log(h_n^{-1}))$ and in the three-dimensional case an accuracy of $O(h_n^2\ (\log(h_n^{-1}))^2)$ can be obtained for sufficiently smooth solutions.

The dimension of the solution space is substantially reduced in comparison to the standard grid approach. In the two-dimensional case we only need $O(h_n^{-1}\log(h_n^{-1}))$ instead of $O(h_n^{-2})$ degrees of freedom. In the case of three-dimensional problems we only need $O(h_n^{-1}\ (\log(h_n^{-1}))^2)$ instead of $O(h_n^{-3})$ degrees of freedom.

There is no need for complicated data structures to represent the sparse grid and no need for sophisticated algorithms to obtain the solution. We just have to solve a

TABLE 10

L_2- and L_∞-norm of the error, full grid on the left, combined solution on the right.

n	$\lvert e_{n,n}\rvert_2$	$\frac{\lvert e_{n-1,n-1}\rvert_2}{\lvert e_{n,n}\rvert_2}$	$\lvert e_{n,n}\rvert_\infty$	$\frac{\lvert e_{n-1,n-1}\rvert_\infty}{\lvert e_{n,n}\rvert_\infty}$	$\lvert e^c_{n,n}\rvert_2$	$\frac{\lvert e^c_{n-1,n-1}\rvert_2}{\lvert e^c_{n,n}\rvert_2}$	$\lvert e^c_{n,n}\rvert_\infty$	$\frac{\lvert e^c_{n-1,n-1}\rvert_\infty}{\lvert e^c_{n,n}\rvert_\infty}$
	$\alpha = 0.125$							
3	2.3171E-3	4.696	4.1210E-3	3.978	3.4773E-3	4.062	1.1681E-2	2.496
4	5.4442E-4	4.256	1.0569E-3	3.899	8.5692E-4	4.058	4.0742E-3	2.876
5					2.2023E-4	3.891	1.4670E-3	2.777
6					6.0845E-5	3.619	4.5330E-4	3.236
7					1.7488E-5	3.479	1.3810E-4	3.282
8					5.0685E-6	3.450	4.1357E-5	3.339
	$\alpha = 0.25$							
3	1.2328E-3	3.408	2.3066E-3	3.351	5.1882E-3	3.594	1.2641E-2	2.267
4	3.2187E-4	3.830	6.5162E-4	3.540	1.4933E-3	3.474	5.9064E-3	2.140
5					5.1843E-4	2.880	2.3389E-3	2.525
6					1.7537E-4	2.956	7.6980E-4	3.038
7					5.6677E-5	3.094	2.7278E-4	2.822
8					1.7737E-5	3.195	8.9370E-5	3.052
	$\alpha = 0.5$							
3	1.7520E-3	4.886	5.9662E-3	3.077	8.5599E-3	2.735	2.8296E-2	1.411
4	3.9924E-4	4.388	1.3116E-3	4.549	2.7436E-3	3.120	1.1184E-2	2.530
5					1.0472E-3	2.620	4.3777E-3	2.555
6					3.3565E-4	3.120	1.6041E-3	2.729
7					1.3102E-4	2.562	6.0695E-4	2.643
8					4.4540E-5	2.942	2.2305E-4	2.721
	$\alpha = 0.75$							
3	2.2734E-3	4.301	7.1804E-3	2.923	1.0241E-2	2.078	3.0782E-2	1.365
4	6.3935E-4	3.556	1.8969E-3	3.785	2.6358E-3	3.885	1.1040E-2	2.788
5					1.0987E-3	2.399	4.4042E-3	2.507
6					3.6211E-4	3.034	1.8599E-3	2.368
7					1.9252E-4	1.881	7.4955E-4	2.481
8					1.7071E-4	1.128	9.6088E-4	0.780
	$\alpha = 1.0$							
3	1.5987E-3	4.360	5.0857E-3	3.151	7.9072E-3	2.567	2.2445E-2	1.809
4	3.7171E-4	4.301	1.2175E-3	4.177	2.8952E-3	2.731	9.1664E-3	2.449
5					1.0115E-3	2.862	3.9667E-3	2.311
6					3.3684E-4	3.003	1.7222E-3	2.303
7					1.0732E-4	3.138	6.3854E-4	2.697
8					3.2960E-5	3.256	2.2181E-4	2.879

couple of regular grid problems $P_{i,j},\ i+j = n, n+1$, with differently scaled mesh sizes. To solve these problems any appropriate method can be used. For reasons of efficiency we recommend multigrid methods (see [3]). For the model problems 1 to 3 we used the HTMG-method (see [2]), a fast implementation of the FAS-scheme. But in general any appropriate method can be applied.

The combination technique can be used together with a commercial finite element package improving its efficiency regarding execution time and in-core memory storage. Additionally, more accurate solutions can now be obtained for a FE-package with limited element number. For the model problems 4 and 5 we used the NISA II code.

Another important aspect of the combination technique is the following: All problems $P_{i,j},\ i+j = n, n+1$, can be solved **fully in parallel**. Synchronization has only to take place for the combination of the different solutions itself.

The results of our experiments have shown that the combination approach can be used even for problems with non-smooth solutions, non-quadratic domain shapes and non-linear operators. Its performance and efficiency have always been superior to the standard grid method. But for non-smooth solutions and more complex problems theory is still missing. Here, like for the standard grid, adaptive refinement seems to be necessary to get a sound solution method. First attempts in this direction are promising.

REFERENCES

[1] H. Bungartz, *An adaptive Poisson solver using hierarchical bases and sparse grids*, this volume.

[2] M. Griebel, *Zur Loesung von Finite-Differenzen- und Finite-Element-Gleichungen mittels der Hierarchischen-Transformations-Mehrgitter-Methode*, TU Muenchen, Institut f. Informatik, TUM-I9007; SFB-Report 342/4/90 A, 1990.

[3] W. Hackbusch, *Multigrid Methods and Applications*, Springer-Verlag, Berlin, Heidelberg, New York, 1985.

[4] P. Hofmann, *Asymptotic expansions of the discretization error of boundary value problems of the laplace equation in rectangular domains*, Numerische Mathematik, 9 (1967), pp. 302–322.

[5] D. Roeschke, *Asymptotische Fehlerentwicklungen beim Laplace-Problem*, Diplomarbeit, TU Muenchen, Institut fuer Informatik, 1991.

[6] C. Zenger, *Sparse grids*, Proc. Conf. GAMM Workshop (Kiel); Notes on Numerical Fluid Mechanics (Vieweg); TUM, Institut f. Informatik, SFB-Report 342/18/90 A, (1990).